Climate Dynamics
https://doi.org/10.1007/s00382-021-05884-9

Intraseasonal variation of rainfall characteristics and latent heating profiles during southwest and northeast monsoon seasons over the Arabian Sea and Bay of Bengal

K. Saikranthi[1] · **N. S. Chiranjeevi**[1]

Received: 20 April 2021 / Accepted: 7 July 2021

Abstract
Recent studies emphasize the significance of precipitation characteristics at intraseasonal time scales for better predicting the monsoonal rainfall. In this connection, to understand the differences in characteristics of the vertical structure of precipitation during wet and dry spells over the Arabian Sea (AS) and Bay of Bengal (BOB) from the southwest monsoon (SWM) to northeast monsoon (NEM) using 16 years of tropical rainfall measuring mission (TRMM) version#7 datasets. On average, the wet and dry spells durations are more during NEM (> 5 days) than SWM (4 days) over BOB, while the durations are identical (5 days) in all spells over AS. Irrespective of the season, shallow systems' occurrence and rain fraction are more in dry spells than the respective wet spells over AS and BOB. During the dry spells of BOB, both rain fraction and occurrence of stratiform and convective rain decreases while shallow rain increases from SWM to NEM. The increase in shallow systems occurrence results bimodal distribution (3 and 5.5 km) in storm height and reflectivity distributions. During wet spells, for different rain types, the occurrence and rain fraction changes are minimal in both seasons and seas. The prevalence of deeper systems than shallow systems is due to changes in atmospheric background conditions from dry to wet spells. The latent heating distributions are broader during SWM than NEM in both spells of two seas. The observed bimodal distribution of latent heating profiles in the dry spells during SWM and NEM over AS, and only during NEM over BOB results from a higher occurrence of shallow rain in these spells.

Keywords Intraseasonal variability · Bay of Bengal · Arabian Sea · Tropical Rainfall Measuring Mission Precipitation Radar (TRMM PR) · Monsoon rainfall · Southwest monsoon · Northeast monsoon · Latent heating

1 Introduction

Southwest monsoon (SWM – June to September) season is considered the worlds' most pronounced and unique weather phenomenon (Rao 1976; Gadgil 2003). Most parts of the Indian subcontinent receive 70–90% of their annual rainfall during the SWM. The northeast monsoon (NEM – October to December) is also equally important, which produce 11% of the annual rainfall throughout India and 30–60% over southern peninsular India (Rajeevan et al. 2012; Misra and Bharadwaj 2019; Radhakrishna et al. 2019; Sengupta and Nigam 2019). The life and economy of India are vulnerable to changes in the monsoonal rainfall; it is of great interest in understanding and predicting the behavior of monsoon dynamics and the variability of the rain at different temporal scales (Webster et al. 1998).

The monsoonal precipitating systems exhibit remarkable variations at intraseasonal, interannual and interdecadal timescales (Webster et al. 1998; Krishnamurthy and Goswami 2000; Goswami et al. 2006; Rajeevan et al. 2012). The intraseasonal oscillations play an important role in modulating the seasonal and interannual rainfall variations (Suhas et al. 2012). Hence, pronounced importance has been given to understand the monsoon intraseasonal variations. These intraseasonal variations are classified into periods with excess rainfall known as wet spells and scanty rainfall denoted as dry spells. Characteristics of wet and dry spells show the duration varies from few days to more than a month, and the trend analysis indicates the

✉ K. Saikranthi
ksaikranthi@gmail.com; saikranthi@iisertirupati.ac.in

[1] Department of Earth and Climate Science, Indian Institute of Science Education and Research (IISER) Tirupati, Tirupati, Andhra Pradesh, India

Published online: 20 July 2021

increasing frequency of short duration spells in recent years (Singh, 2013). At intraseasonal time scales, rainfall shows three modes of oscillations (3–8 day; 10–20 day and 30–60 day) over India (Goswami et al. 2006; Rajeevan et al. 2010; Radhakrishna et al. 2019). The propagation direction of precipitating systems differs from one mode to other over the equatorial Indian Ocean. For instance, the precipitating systems propagate northward during 10–20 day oscillations and northwestward during 30–60 day oscillations, and the precipitating systems originated over the Arabian Sea (AS) and Bay of Bengal (BOB) play a significant role in the monsoonal rainfall over India landmass (Krishnan et al. 2000; Chattopdhyay et al. 2009; Pathak et al. 2017; Karmakar et al. 2017; Karmakar and Krishnamurthi 2019; Karmakar and Misra 2020).

Monsoon systems are land-atmosphere-ocean coupled systems; it is vital to know the morphology of precipitation over the AS and BOB along with the Indian landmass for their better representation in the climate models (Mukhopadhyay et al. 2010; Sabeerali et al. 2013; Ajayamohan et al. 2016). Using the tropical rainfall measuring mission (TRMM) precipitation radar (PR) data and model outputs, Chattopadhyay et al. (2009) showed that the convective rain exhibits weak northward propagation, while organized stratiform strongly modulates the northward propagation. They also emphasized the impact of latent heating at different heights during the stratiform rain on the northward propagation. Thus, the information of stratiform and convective precipitation is vital for simulating the northward propagation in the climate models during wet and dry spells. Rowe et al. (2019) emphasized the importance of rain microphysical processes for simulating accurate rainfall at intraseasonal timescales over the Indian Ocean. The studies mentioned above on the propagating systems portray the need to understand the vertical structure of precipitating systems originated over the AS and BOB and associated latent heating profiles at intraseasonal timescales for better predicting the monsoonal rainfall over the India landmass.

The occurrence and vertical structure of different types of precipitation over India and surrounded seas during different seasons (Rajeevan et al. 2010; Romatschke et al. 2010; Romatschke and Houze 2011; Saikranthi et al. 2013, 2014; Bhat and Kumar 2015; Rao et al. 2016; Phadtare and Bhat 2019) and in El Niño and La Niña episodes (Saikranthi et al. 2018) have been well documented over the Indian region. Over open oceans, sea surface temperature (SST) being the driving force for convective initiation, its link with clouds occurrence (Nair and Rajeev 2014), convection (Gadgil et al. 1984), and different types of precipitating systems and vertical structure (Saikranthi et al. 2019a, b) have been studied over the Indian Ocean during the SWM. However, the vertical structure information and their association with the background atmosphere at intraseasonal timescales are less known over the AS and BOB in SWM and least explored during NEM. Hence, the present study aims to understand the following:

1. Do the intraseasonal variations (i.e., in wet and dry spells) of precipitating systems are similar or not in SWM and NEM over AS and BOB?
2. Is the vertical structure of precipitation (in terms of vertical profiles of reflectivity and storm height) and associated latent heating profiles differ at intraseasonal timescales during the SWM and NEM over the AS and BOB?
3. The effect of atmospheric background conditions prevailing during SWM and NEM at intraseasonal timescales over the two seasons on the variations in the morphology of precipitating systems.

2 Data and methodology

TRMM-PR products 2A25, 2H25, and 3B42 version#7 datasets have been used from 1998 to 2013 over the AS (8–20 °N and 63–72 °E) and BOB (8–21 °N and 83–92 °E) in the SWM and NEM seasons. To get rid of the range height offset issues (Houze et al. 2007, 2015), instead of TRMM-PR 2A25 and 2H25 data products, the three-dimensional gridded reflectivity and latent heating profiles are used. For the reflectivity profiles, the spatial resolutions of the gridded data are 0.05° and with a vertical resolution of 0.25 km. Latent heating data is available at 19 levels with a vertical resolution of 0.5 km for the first three levels and 1 km thereafter. The reflectivity profiles are segregated into convective, stratiform, and shallow rain using the TRMM-PR 2A23 classification outcome (Awaka et al. 2009). Based on the horizontal and vertical extent, Houze et al. (2007) further classified these profiles into deep convective cores (DCC), deep wide convective cores (DWC), wide convective cores (WCC), broad stratiform regions (BSR), and isolated shallow echoes (ISE). Systems identified on moderate thresholds are used in this study, i.e., DCC - intensity $\geq$ 30 dBZ & storm height $\geq$ 8 km, WCC - intensity $\geq$ 30 dBZ & horizontal contiguous area $\geq$ 800 km^2, DWC are echoes satisfying both DCC and WCC thresholds, BSR $-$ 2A23 stratiform contiguous area $\geq$ 40,000 km^2, ISE - storm height $\leq$ freezing level height by at least 1 km. Furthermore, TTRMM-PR 2H25 spectral latent heating data (Shige et al. 2004; Tao et al. 2006) is derived from radar estimated stratiform and convective rain intensity and other characteristics of echoes within the range of the radar.

ERA5 is a successor of the ERA-Interim reanalysis and is the fifth generation reanalysis from the European centre for medium-range weather forecasting (ECMWF, Copernicus Climate Change Service (C3S) 2017). The spatiotemporal

resolution of ERA5 data used in the present study is 1° × 1° and 1 h, respectively. The total column water vapor, temperature, relative humidity, and vertical velocity datasets are considered from the ERA5 reanalysis. The equivalent potential temperature (θ_e) is calculated using the formula given in Wallace and Hobbs (2006):

$$\theta_e = \theta \exp\left(\frac{L_v w_s}{C_p T}\right) \quad (1)$$

where θ, L_v, w_s, C_p and T represent the potential temperature, latent heat of vaporization, saturation mixing ratio, specific heat at constant pressure, and absolute temperature, respectively. The SST dataset utilized in this study has taken from the national oceanic and atmospheric administration (NOAA) optimum interpolation SST (OISST) generated using the datasets from different kinds of platforms like satellites, ships, and buoys (Reynolds et al. 2007). The spatiotemporal resolution of the OISST dataset is 0.25° × 0.25° and 1 day.

The wet and dry spells are identified using the rainfall data from the TRMM 3B42. This data product consists of three hourly rainfall estimates with a spatial resolution of 0.25° × 0.25°. Daily rainfall is estimated from the 3 h data during the SWM and NEM over both seasons. Later, the standardized rainfall anomaly for each day has been calculated using the formula given below:

$$\textit{Standardized rainfall anomaly}\,(SRA) = \frac{r-\mu}{\sigma} \quad (2)$$

where *SRA* represents standardized rainfall anomaly, r be the spatially averaged daily rainfall for a particular day in a given year, μ indicates the mean of average daily rainfall for all the years of a specific day, and σ represents the standard deviation of average daily rainfall for all the years of a particular day. If the *SRA* for each day is >0.5 (<-0.5) for at least three consecutive days, then it is classified as a wet (dry) spell following Singh and Nakamura (2010), Shrestha et al. (2012), and Rao et al. (2016). In addition to these days, consecutive days having $SRA > 0.25$ or $SRA < -0.25$ in the mid of the spell are added to wet and dry spells, respectively.

3 Results

The wet and dry spells during NEM and SWM are identified, and the distributions of spell durations and accumulated rain over the AS and BOB are shown in Fig. 1. Regardless of the season, the duration of dry and wet spells is more over AS than the respective spell over BOB (Fig. 1a, b). However, a contrary feature is observed in accumulated rain during the respective spells (Fig. 1c, d), i.e., rainfall is more in BOB than in AS in the respective cells. The duration of the spells of both seasons is the same over AS. Over BOB, the duration is more in dry spells of NEM than in the other three spells, which show the same value. Accumulated rain is more in spells of SWM than in the respective spells of NEM over both AS and BOB. A broader distribution of duration of spells is seen in dry spells than in wet spells of both seasons.

3.1 Occurrence and rain fraction of different rain types

The variations in the occurrence of convective, stratiform, and shallow rain could result in differences in the accumulated rainfall (Fig. 1c, d). To study the observed variations in accumulated precipitation in different spells, the occurrence and rain fraction of convective, stratiform, and shallow rain are calculated for each spell and depicted in Fig. 2. Rain fraction of a particular rain type is the contribution of rain by that rain type to the total accumulated rainfall in a given spell and season. The occurrence of stratiform rain is more in the wet spells, whereas convective and shallow rain is more in the dry spells during both seasons. The occurrence of stratiform and convective (shallow) rain is more (less) over the BOB than the AS in both spells. The increase in the occurrence of shallow rain is prominent over the BOB during the dry spells from SWM (20%) to NEM (33%) (Fig. 2a, b). Though the occurrence of convective rain is less, its contribution to the rain fraction is more than the other types of rainfall (except for shallow rain over the AS during the dry spell) during both seasons. Like the occurrence, the rain fraction of convective and shallow rain (stratiform rain) is also more (less) in the dry spells than in the wet spells during both seasons. To further examine these convective, stratiform, and shallow rain are produced from which type of precipitating systems, the percentage occurrence of DCC, DWC, WCC, BSR, and ISE during wet and dry spells over the AS and BOB are shown in Fig. 3. The occurrence and rain fraction of deeper precipitating systems (DCC, DWC, WCC, and BSR) are more and isolated shallow systems are less in the BOB than in the AS during both the spells of SWM. While in the NEM, the occurrence and rain fraction of DCC, DWC, and ISE are more, and BSR is less over the AS than the BOB. Regardless of the season and region, the occurrence and rain fraction of BSR and DWC are more, and ISE is less during wet spells than the dry spells, indicating large scale systems during wet spells and isolated shallow systems in dry spells. Further, both occurrence and rain fraction of BSR and DWC are increasing, and ISE decreases in dry spells from SWM to NEM over BOB. It is interesting to note that in both the spells, the occurrence and rain fraction of DWC are more over the BOB than the AS during SWM, while the contrary feature is evident during the NEM (Fig. 3).

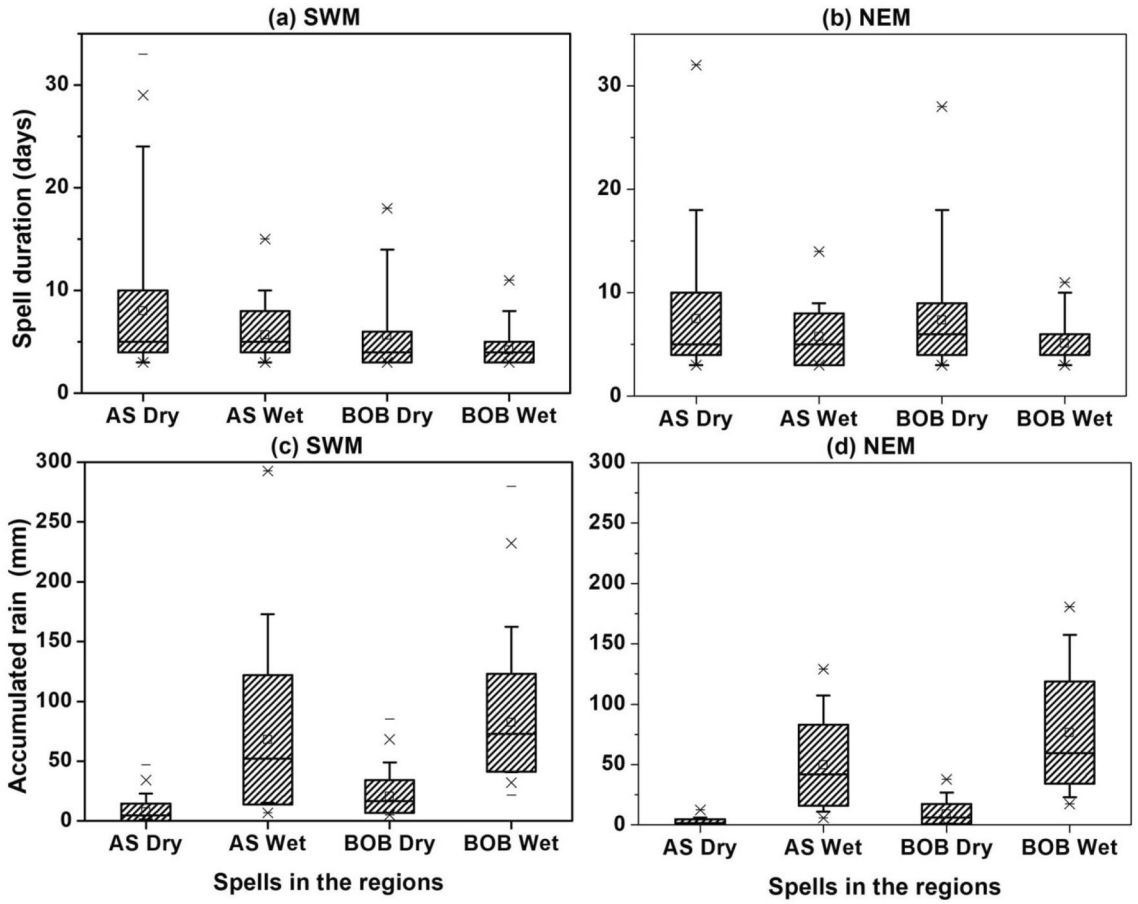

Fig. 1 **a**, **b** Represents the distribution of duration in the wet and dry spells during the SWM and NEM season over the BOB and the AS respectively. **c**, **d** Are same as **a** and **b**, respectively, but for the accumulated rain during the spells

Saikranthi et al. (2018) showed that the occurrence and intensity of convective, stratiform, and shallow rain vary during ENSO conditions. To further know the differences of these rain types during El Niño and La Niña conditions, the anomalies of occurrence and rain fraction of convective, stratiform, and shallow rain are plotted during wet and dry spells of SWM and NEM in Fig. 4. ENSO index is considered from Niño 3.4 that averages the SST anomalies between 5 °N–5 °S, 120 °W–170 °W. During the TRMM era, Niño 3.4 index segregated 2002, 2004, and 2009 as El Niño years and 1998, 1999, 2000, 2007, and 2010 as La Niña years (Saikranthi et al. 2018). The climatological occurrence of convective, stratiform, and shallow rain is subtracted from the respective rain type occurrence during the ENSO episodes to calculate the anomalies. The positive values indicate more occurrences in ENSO episodes than climatology and vice versa. During the dry spells, the occurrence and rain fraction of deep systems (convective and stratiform) increase, and shallow systems decrease in NEM El Niño episodes and vice versa in La Niña episodes over AS. The occurrence and rain fraction of shallow rain increase and stratiform rain decrease in ENSO episodes during wet spells, while convective rain increases in El Niño and no variations in La Niña episodes of both monsoon seasons over the AS. The variations in the occurrence and rain fractions are minimal during the wet spells of La Niña episodes over BOB, while dry spells show considerable variations. During the wet spells of El Niño episodes over BOB, the occurrence of convective rain increases in NEM and almost no variation in SWM, whereas stratiform rain decreases considerably and shallow rain increases during both seasons. The increased occurrence of convective rain and decreased stratiform rain with decreased rain fraction during NEM dry spells over BOB indicate the more occurrence feeble isolated convective storms in El Niño episodes. During La Niña episodes, deep rain occurrence and rain fraction decreases, and shallow rain increase over the BOB.

3.2 Vertical structure of precipitation

To elucidate the vertical structure of precipitation in the wet and dry spells, the contour frequency by altitude

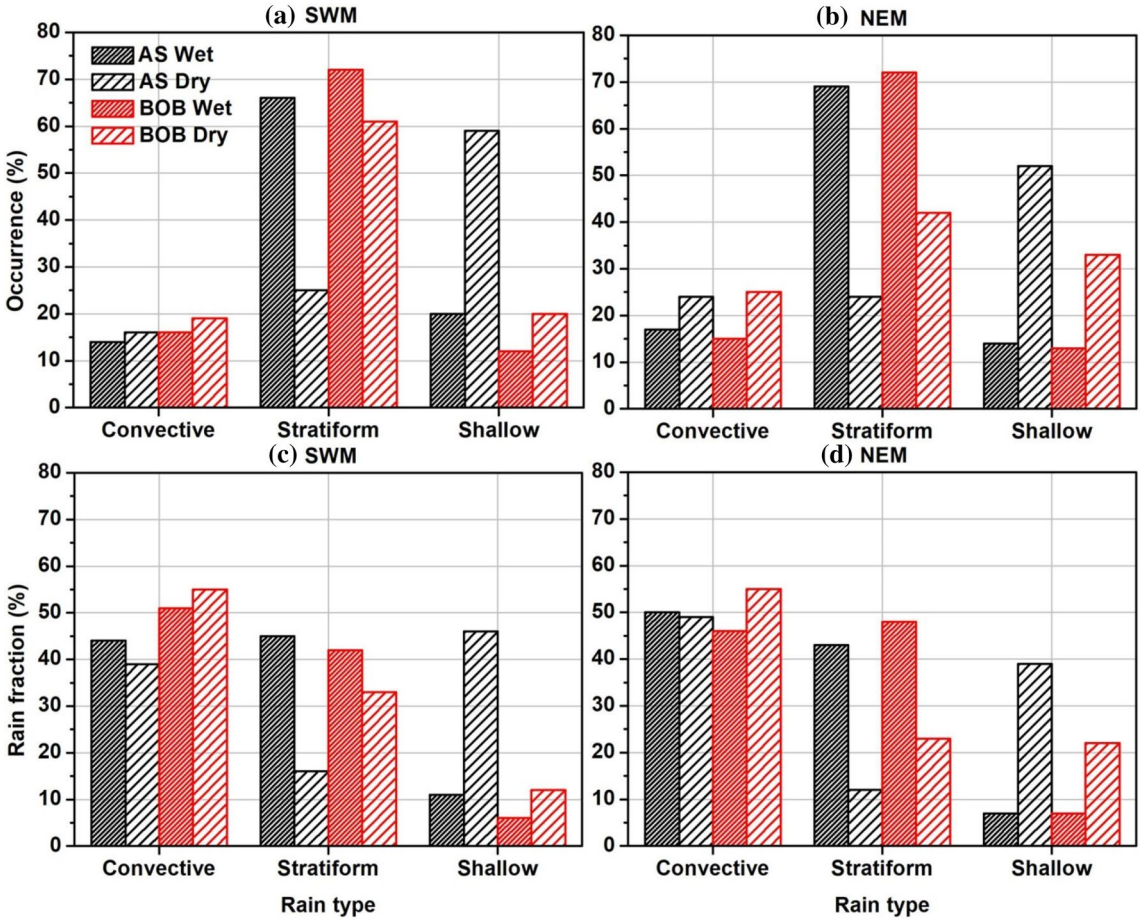

Fig. 2 **a** Occurrence of convective, stratiform, and shallow rain in the wet and dry spells during the SWM season over the BOB and the AS. **b** Same as **a** but for NEM season. **c**, **d** Are same as **a** and **b**, respectively, but for the rain fraction

diagrams (CFADs) of reflectivity (in dBZ) are constructed following Rao et al. (2016) over the AS and the BOB during the SWM and NEM and are depicted in Fig. 5. The large occurrence of reflectivity below 4 km altitude in the dry spells over the AS during both the seasons and dry spells of BOB during NEM indicates shallow rain prevalence in those spells (also seen from Figs. 2 and 3). Except in the dry spell of SWM over the AS, reflectivity distribution shows the predominance of deep (convective and stratiform) rain. Irrespective of the spells, the occurrence of shallow rain is copious over the AS during the SWM. The reflectivity distributions in the respective spells below 4 km altitude show larger values in the NEM than in the SWM. Thus in a given spell, the occurrence of shallow rain is abundant in NEM than in SWM (Figs. 2a, b and 3a, b). The CFADs of reflectivity also show broader distributions in the wet spells than the dry spells during both seasons. The median reflectivity profiles (Fig. 5e, j) are the same for the wet spells and the dry spells separately over both the seas during the NEM. However during SWM, below the melting layer, the median reflectivity values are larger in the dry spells over the BOB than the AS and are nearly the same in the wet spells.

The distributions of storm heights (the topmost height of the reflectivity profile with three consecutive lower range bins having conditional reflectivity values ≥ 17 dBZ; Saikranthi et al. 2014; and Rao et al. 2016) are computed in the wet and dry spells of SWM and NEM and are depicted in Fig. 6. The storm height distributions are distinctly different for dry and wet spells over the AS during both seasons. However, the distributions are identical over the BOB during the SWM and show large variations during the NEM. The occurrence of deep systems decreases and shallow systems increase substantially during the dry spells of NEM over the BOB, which results in a pronounced peak at 3 km (Fig. 6b). The storm height peak observed at 3 km altitude over the AS during SWM and over both the seas in the dry spells of NEM also confirms the predominance of shallow rain in those spells. The other peak seen at ~ 6 km altitude is due to stratiform rain occurrence with feeble echoes at the upper heights for which TRMM-PR is not sensitive (Saikranthi et al. 2014). The storm height distributions show

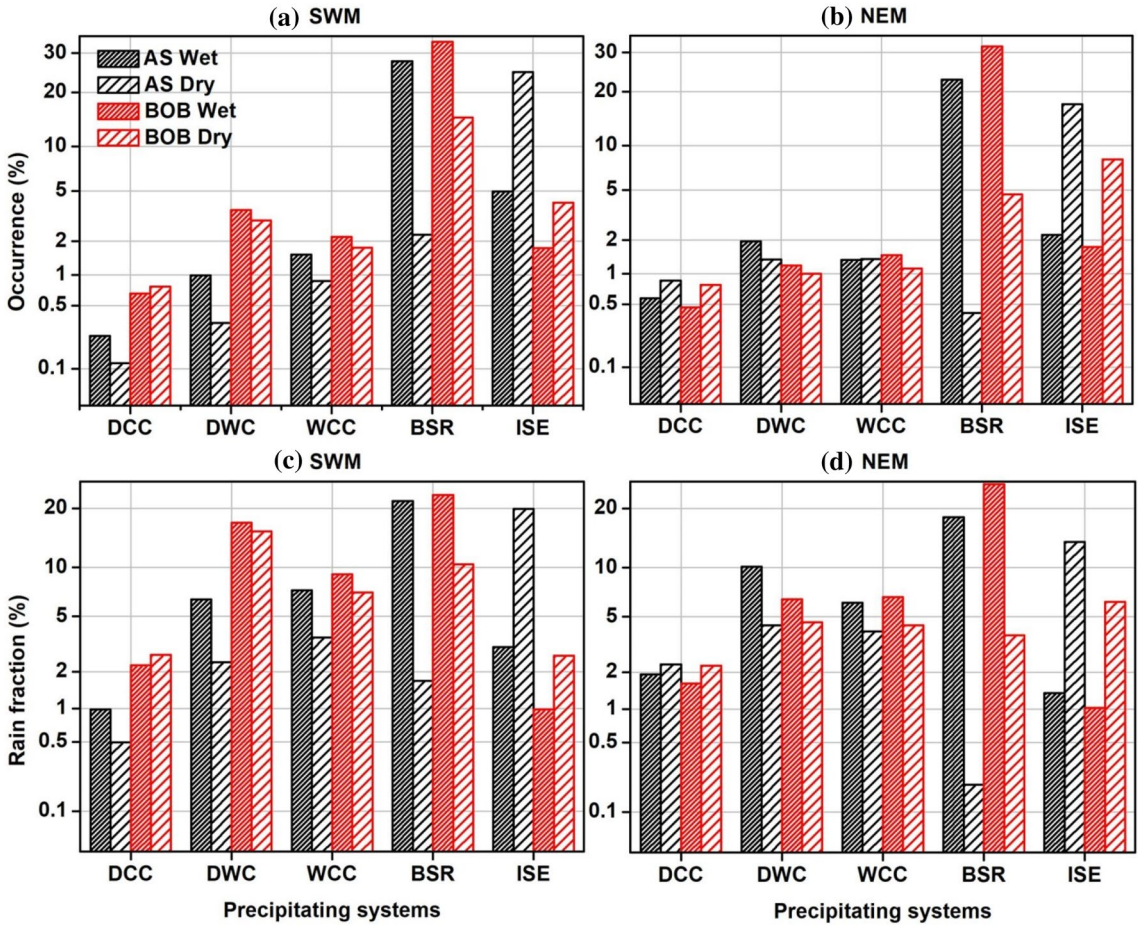

Fig. 3 **a** Occurrence of deep convective cores (DCC), deep wide convective cores (DWC), wide convective cores (WCC), broad stratiform regions (BSR), and isolated shallow echoes (ISE) in the wet and dry spells during the SWM season over the BOB and the AS. **b** Same as **a** but for NEM season. **c**, **d** Are same as **a** and **b**, respectively, but for the rain fraction

bimodality over BOB in the dry spells of NEM. The storm height distributions confirm that the occurrence of the deep systems is more in the wet spells than in the dry spells over both the seas. Irrespective of the spell, the occurrence of deep systems is more and shallow systems is less over BOB than over AS.

3.3 Latent heating structure

An increase of 1 mm h^{-1} in rain rate produces 3.5 K h^{-1} more vertical integrated latent heating (Zagrodnik and Jiang 2014). Thus, the latent heating profile depends on the vertical profile of reflectivity and rain type. As the vertical structure of precipitation changes during wet and dry spells over AS and BOB, one can expect that there should be a change in the vertical structure of latent heating profiles. To examine the differences in latent heating structure, CFADs of latent heating profiles are constructed with 1 K h^{-1} interval in wet and dry spells of SWM and NEM and are shown in Fig. 7. Irrespective of seasons, the latent heating distribution is broader at all heights during wet spells than in dry spells. Comparing the two basins, the latent heating distributions are broader over BOB than AS in respective spells of both seasons. The latent heating distribution is narrower in NEM than SWM over both AS and BOB in a given spell. The broader distribution of latent heating indicates the wider distribution of reflectivities (rain intensities). The median latent heating profiles (Fig. 7e, j) show negative values below 4 km altitude except during dry spells of SWM and NEM over AS and dry spells of NEM over BOB. The predominant occurrence of stratiform rain in other spells and shallow rain in the three spells mentioned above (Fig. 3) results in the observed variations of the latent heating profiles. As shown in Liu et al. (2015) and the references therein, the latent heating is absorbed (negative) due to evaporation below the melting layer in stratiform rain and released (positive) at all heights in convective precipitation due to condensation and vapor deposition below and above melting layer, respectively. The predominance of shallow rain over tropical oceans results in two modes in the vertical distribution of latent heating

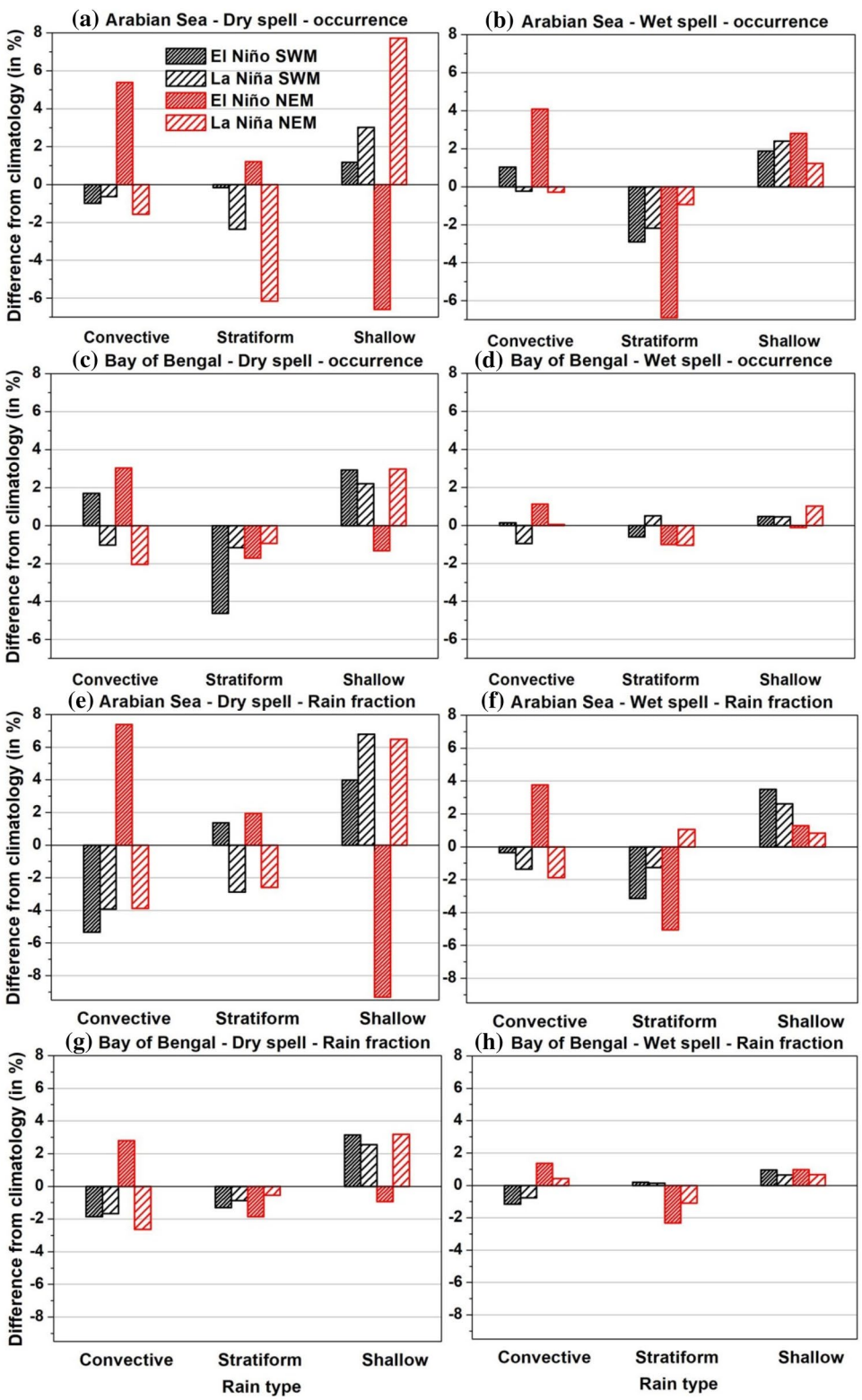

Fig. 4 **a**, **b** Anomaly of occurrence of convective, stratiform, and shallow rain during El Niño and La Niña years of SWM and NEM for dry and wet spells over AS. **c**, **d** Is same as **a** and **b** but over BOB. **e**–**h** Are same as **a**–**d** but for rain fraction respectively

profiles (Liu et al. 2015), as seen in the dry spells over the AS and dry spells of NEM over the BOB. The observed large values (around 8 km altitude) of latent heating follow the storm height distributions shown in Fig. 6. Latent heating profiles also indicate the presence of deeper and intense systems except in the dry spells of NEM over both the seas and dry spells of SWM over the AS.

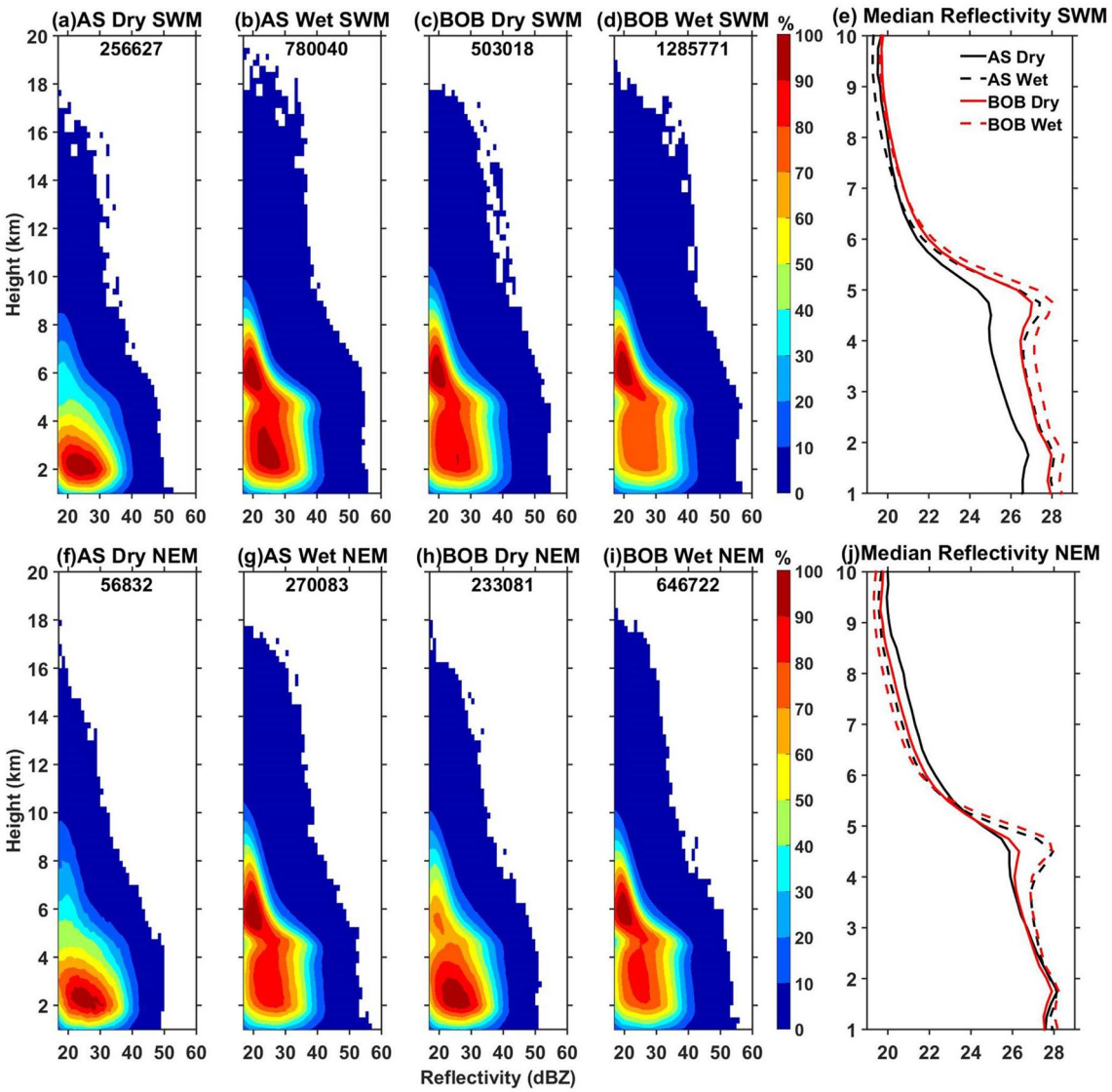

Fig. 5 **a**, **c** Are the CFADs of reflectivity (dBZ) in the dry periods over the AS and the BOB, respectively, during the SWM season. **b**, **d** Are same as **a** and **c** but for wet periods. **f**–**i** Are same as **a**–**d**, respectively, but for NEM season. **e**, **j** Represents the median reflectivity profile during SWM and NEM respectively

3.4 Background atmospheric conditions

The variations observed in the occurrence of different kinds of precipitating systems during the dry and wet spells of SWM and NEM over the AS and BOB could be due to the differences in the surface forcing (SST) and/or the atmospheric background conditions (Chen et al. 2015; Saikranthi et al. 2018, 2019b; Radhakrishna and Rao 2021). Atmospheric background conditions also alter the monsoonal rainfall over India (Hazra et al. 2020). To check the role of surface forcing on the occurrence of various kinds of precipitating systems, the distributions of SST in wet and dry spells of SWM and NEM over the AS and BOB are plotted in Fig. 8. The SST distributions are identical in the dry and wet spells of BOB during both seasons, while the occurrence of larger SSTs is more and smaller SSTs are less in the wet spells than in the dry spells over the AS during SWM. On the other hand, the distributions are similar for dry and wet spells over the AS during the NEM. Regardless of the spells and seasons, SSTs are larger over the BOB than over the AS, indicating larger surface forcing over the BOB than AS in both the monsoon seasons. Intercomparison of spells show the same surface forcings in dry and wet spells over the BOB and show smaller values in the dry spells than in wet spells over the AS during the SWM. On the other hand, the surface forcing is the same for the dry and wet spells over both the AS and BOB during the NEM.

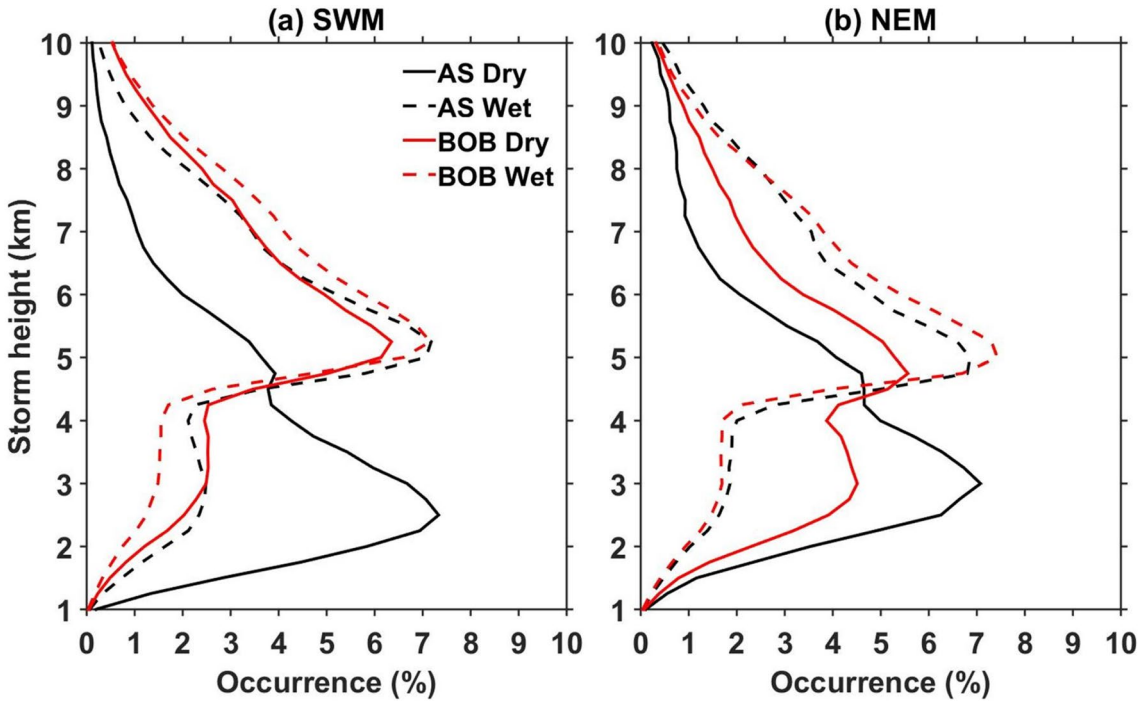

Fig. 6 **a** Distribution of conditional reflectivity (≥ 17 dBZ) echo top altitude with height in the wet and dry periods during the SWM over the AS and the BOB. **b** Same as **a** but during the NEM season

Precipitating system size and vertical extent depend not only on the surface forcing but also on the background atmospheric conditions (Chen et al. 2015; Radhakrishna and Rao 2021) like the total column water vapor (TCWV), equivalent potential temperature (θ_e), relative humidity (RH), and vertical velocity. The distributions of TCWV during dry and wet spells of SWM and NEM are plotted in Fig. 9. Overall, the TCWV values are larger in the wet spells than dry spells over both the seas and seasons. During SWM, TCWV distributions are alike over the AS and BOB in the wet spells and possesses larger values over the BOB than AS in dry spells. TCWV values are larger in both dry and wet spells over the BOB than AS during NEM.

To know the stability of the air parcel at different altitudes, the mean vertical profiles of θ_e, for the available moisture mean profiles of RH, and for the dynamical effects, the mean profiles of vertical wind are computed in the respective spells and seasons and are plotted in Fig. 10. The surface θ_e is the same for wet and dry spells over the AS and BOB; however, the values are larger over the BOB than AS during the SWM. Irrespective of the spell and region, the surface θ_e is the same during the NEM. The gradients of θ_e clearly show (Fig. 10a) the presence of stable layers between 900 and 800 hPa levels in the dry spells over the AS, and such stable layers are absent in the wet spells during the SWM. These stable layers are not present over the BOB (Fig. 10a, b) during both the seasons and in NEM over the AS (Fig. 10b). The positive gradients in θ_e indicate the presence of stable layers (Saikranthi et al. 2019b). The presence of stable layers obstruct the vertical growth of precipitating systems as the air parcel requires sufficiently high energy (more than the strength of stable layer) to penetrate in to deeper levels. Thus, over tropical oceans where stable layers are present, the occurrence of shallow systems increases (Shige and Kummerow 2016; Saikranthi et al. 2019b). The vertical distribution of RH depicts distinctly different features in the dry and wet spells during both seasons (Fig. 10c, d). The lower- and mid-troposphere are relatively drier in the dry spells than in the wet spells. Regardless of the spell, the relative humidity is larger over the BOB than over the AS. The mid-troposphere is driest over the AS during SWM and over both the regions during NEM. The mean vertical wind depicted in Figs. 10e, f shows an upward wind during the wet spells. In dry spells, a downward motion is seen in the mid-troposphere over the AS, and an upward motion is seen at all levels during SWM over both regions. A downward motion during the dry spells and upward motion during the wet spells is observed at all levels in the NEM. The strength of upward motion is large (> 0.06 Pa s^{-1} in SWM over BOB and > 0.03 Pa s^{-1} over AS in NEM) during the wet spells, and downward motion is small during the dry spells over the BOB (~ 0.01 Pa s^{-1}) than over the AS (~ 0.02 Pa s^{-1}).

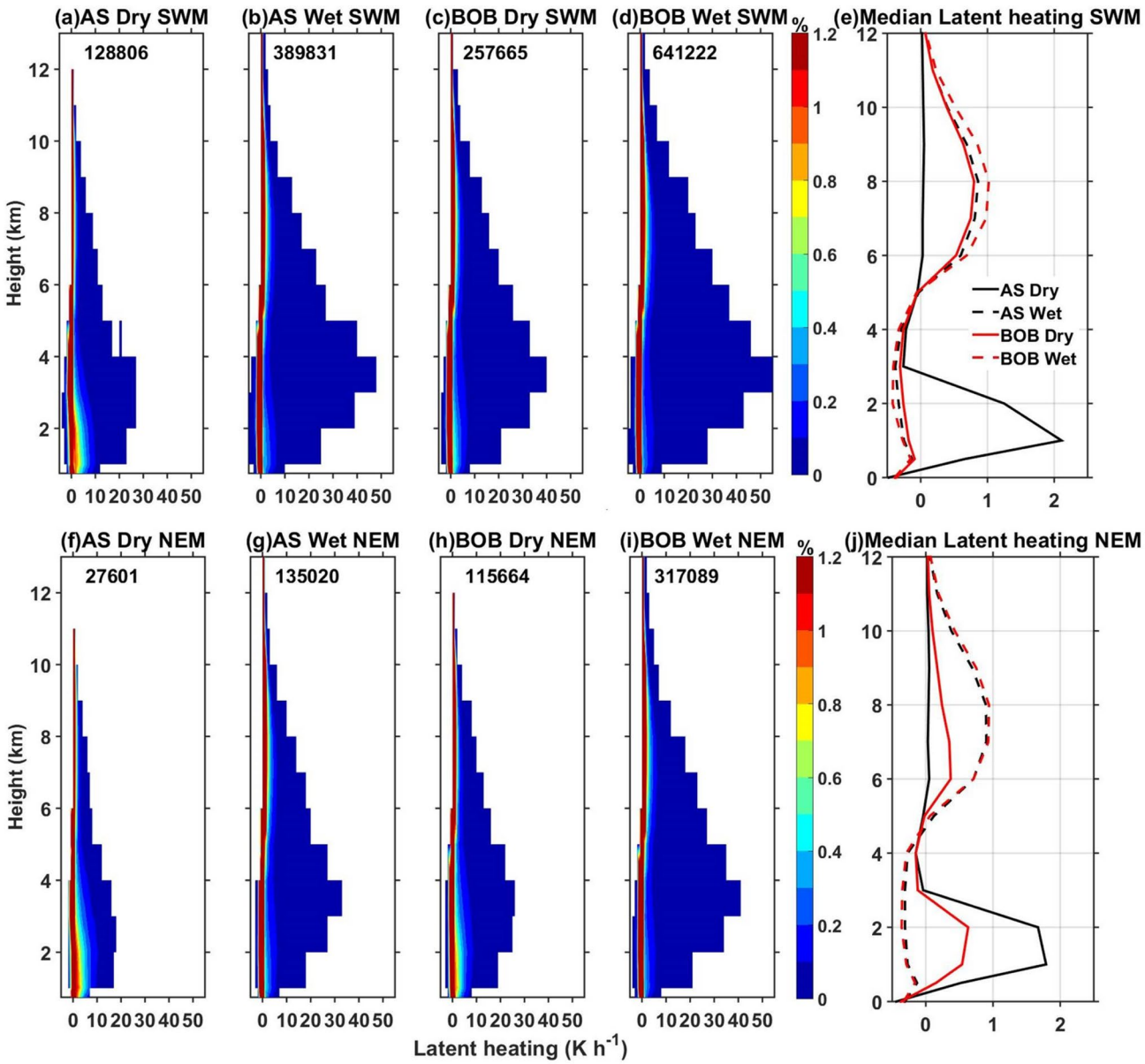

Fig. 7 **a**, **c** Are the CFADs of latent heating (K h^{-1}) in the dry periods over the AS and the BOB, respectively, during the SWM season. **b**, **d** Are same as **a** and **c** but for wet periods. **f–i** Are same as **a–d**, respectively, but for NEM season. **e**, **j** Represents the median latent heating profile during SWM and NEM respectively

4 Association of precipitating systems with background atmospheric conditions

4.1 Dry spells of AS

The dry spells of AS during SWM have less surface forcing, low TCWV values, strong inversion layers below 800 hPa level, dry mid-troposphere, and downward vertical wind in the mid-troposphere. However, the NEM dry spells have less surface forcing, the lowest TCWV values, driest mid-troposphere, and prevailing downward vertical wind across all the heights. As shown in Chen et al. (2015), small-scale systems will form in the presence of less surface forcing and low TCWV values. These systems' vertical growth is strongly retarded by the inversion layers and downward motion and precipitates as shallow rain. Thus, the occurrence of shallow rain is dominant in both seasons over the AS (Fig. 2). As the inversion layers are nearly absent during the NEM, the shallow rain occurrence is relatively less in the NEM than SWM. The less occurrence of stratiform rain also confirms the presence of more small-scale systems in the dry spells, which is in accordance with the findings of Chen

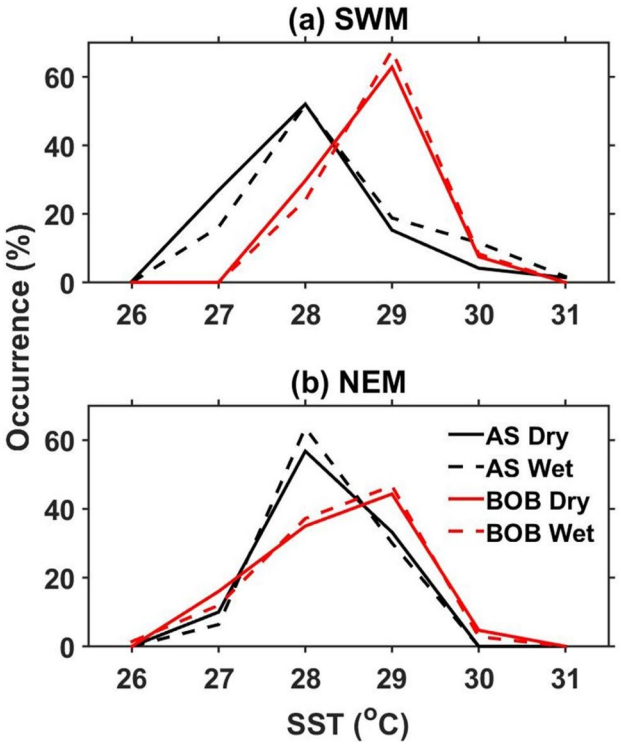

Fig. 8 **a** Distribution of SST (°C) in the wet and dry periods during the SWM over the AS and the BOB. **b** Same as **a** but during the NEM season

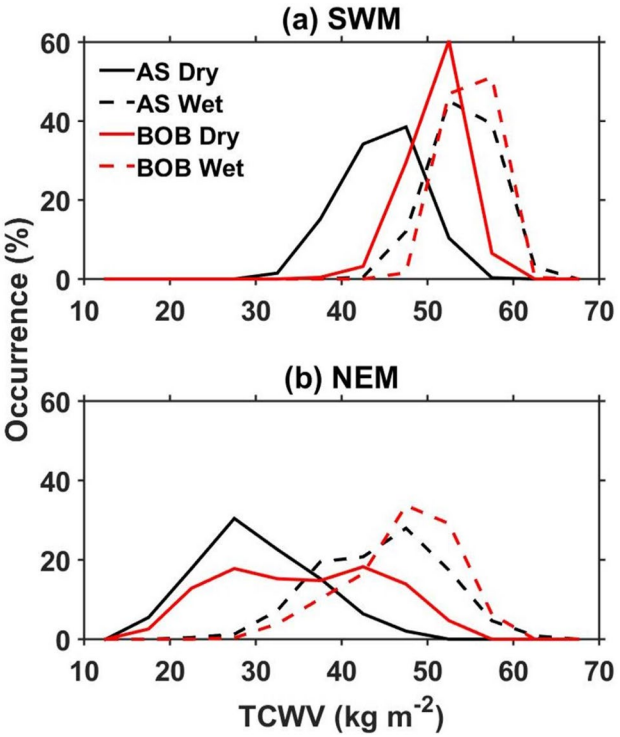

Fig. 9 **a** Distribution of TCWV (kg m^{-2}) in the wet and dry periods during the SWM over the AS and the BOB. **b** Same as **a** but during the NEM season

et al. (2015). Saikranthi et al. (2018, 2019a) showed that the occurrence of shallow systems decrease, and deep systems increase with the increase in SST. As SST increases, the surface forcing increases, TCWV increases, the occurrence of inversion layers decreases, and the mid-troposphere becomes moist, which favors the vertical and horizontal growth of precipitating systems (Saikranthi et al. 2018, 2019b). Therefore, the deep convective and stratiform rain occurrence is possible at SSTs greater than 28 °C.

4.2 Wet Spells of AS

The wet spells of AS during SWM possess larger SSTs indicating enormous surface forcing, larger TCWV values, moist troposphere, and upward vertical wind than the dry spells. Also, the temperature inversions present in the dry spells are nearly absent in the wet spell periods. Nonetheless, the NEM have approximately the same surface forcing, larger TCWV values, moist troposphere, and upwards vertical wind than the dry spells. The moist mid-troposphere, larger TCWV values, and upward motion favor the growth of precipitating systems both in horizontal and vertical dimensions and produce large-scale systems (Chen et al. 2015; Radhakrishna and Rao 2021). This is evidenced from the considerable increase in the occurrence of stratiform (~5%) rain and decrease in the occurrence of shallow (~8 %) rain (Fig. 2) than the respective dry spells.

4.3 Dry spells of BOB

The dry spells of SWM over BOB show large surface forcing, moderate TCWV, moist mid-troposphere, and weak upward vertical wind at all levels. However, the NEM also shows large surface forcing, weak to moderate TCWV, dry mid-troposphere, and small downward vertical wind at all levels. The temperature inversions are nearly absent in the lower troposphere in both seasons. Large surface forcing and moderate TCWV values favor the formation of large-scale systems, while the moist mid-troposphere and upward vertical winds allow the systems to grow to deeper heights in SWM, and the dry mid-troposphere and downward vertical wind inhibit the vertical growth in NEM. As evidenced from Fig. 2, this results in relatively more (~18%) occurrence of stratiform rain and less (~13%) shallow rain in the SWM than in the NEM.

Intercomparison of atmospheric parameters over the AS and BOB reveals that the dry spells of BOB show larger TCWV values, more moisture in the mid-troposphere, small upward motion instead of downward motion in the mid-troposphere, and nearly no inversions in the lower troposphere

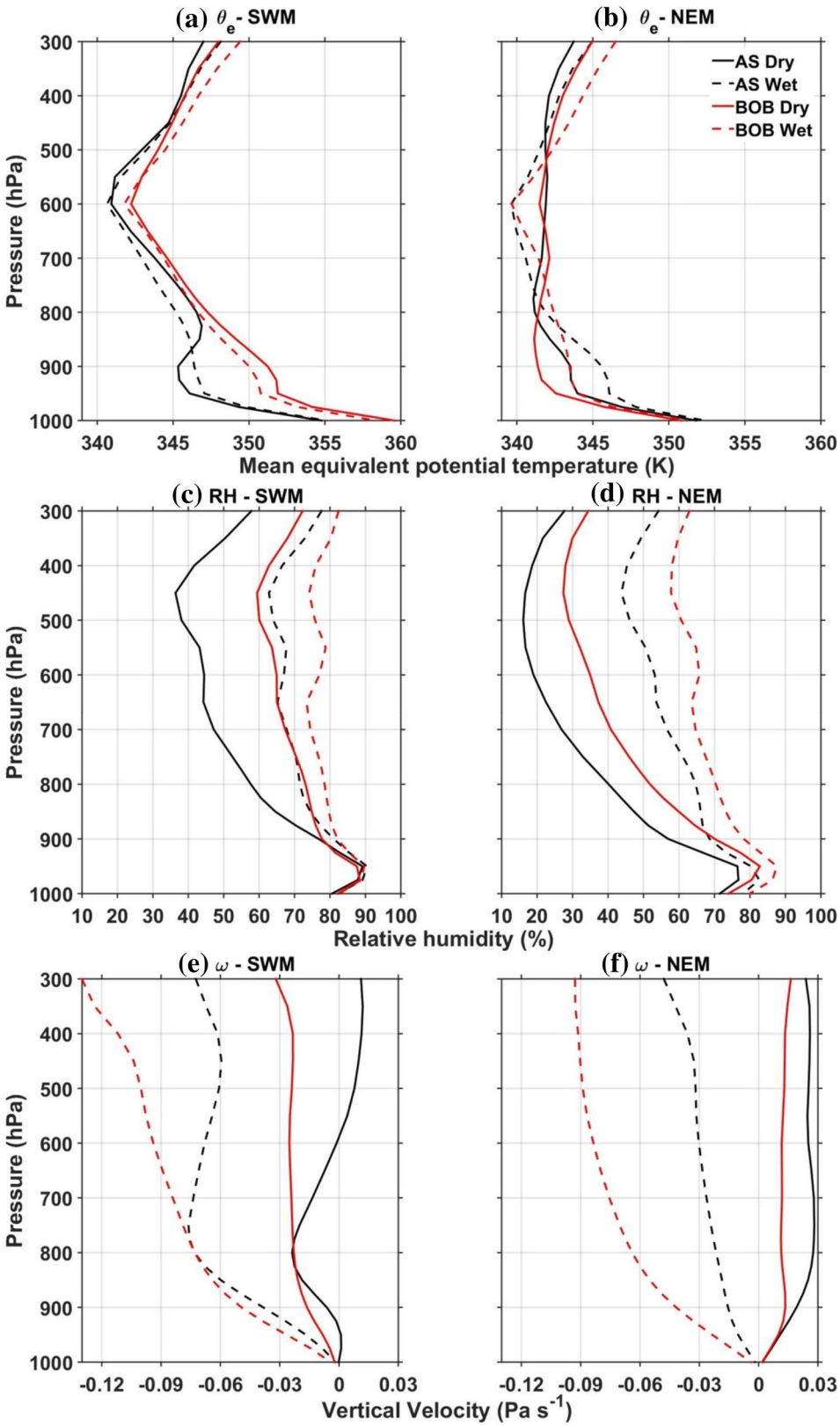

Fig. 10 **a** Vertical profiles of mean θ_e (K) in the wet and dry periods during the SWM over the AS and the BOB. **b** Same as **a** but during the NEM season. **c**, **d** Are same as **a** and **b** respectively but for RH (%). **e**, **f** Are same as **a** and **b** respectively but for vertical wind (Pa s^{-1})

than the AS. Hence, the occurrence of stratiform rain is more (~36% in SWM & ~17% in NEM), and shallow rain is less (~39% in SWM & ~19% in NEM) over the BOB than over the AS (Fig. 2).

4.4 Wet Spells of BOB

BOB wet spells during both seasons possess large surface forcing, largest TCWV values, moist mid-troposphere, strong upward vertical wind, and no inversions layers in the lower troposphere. All these atmospheric conditions favor the formation of large-scale systems that results in a significant occurrence of stratiform rain and lesser occurrence of shallow rain, as evidenced in Fig. 2. Since the background atmospheric conditions are similar in both seasons, the occurrence of different kinds of rainfall (convective, stratiform, and shallow) is also the same during the wet spells.

As evidenced from Fig. 8, the surface forcing differs slightly from SWM to NEM but similar for the dry and wet episodes in each season. Hence, the differences observed between dry and wet spells are due to atmospheric background parameters over the BOB. The arid mid-troposphere in the dry spells of NEM is the major cause for the observed large occurrence of shallow rain (Fig. 2), which is not frequent over the BOB.

5 Conclusions

TRMM-PR (1998–2013) dataset is used to study the variation of rain types, vertical structure of precipitation and latent heating structures over AS and BOB during the wet and dry spells of SWM and NEM. The augmented ERA5 reanalysis data are used to know the association of background atmospheric conditions with the observed variations in precipitating systems. The intraseasonal variations during SWM are distinct from NEM over two seas. This analysis reveals the following:

- The average durations of wet and dry spells are more in NEM than SWM over the BOB, while the mean durations are the same in all spells over the AS.
- Regardless of the season, shallow systems (ISEs) occurrence and rain fraction are more in dry spells than wet spells over AS and BOB. In concurrence with this, the storm height and reflectivity distribution also show higher occurrence around 3 km altitude.
- During the dry spells of AS, the observed dry mid-troposphere, small TCWV, downdrafts in the lower and mid-troposphere, and presence of stable layers in the lower troposphere retard the vertical growth of precipitating systems that result in isolated shallow systems.
- In the dry spells of BOB, both rain fraction and occurrence of stratiform and convective (DWC) rain decreases while shallow systems increases from SWM to NEM. The shallow systems increase result in bimodal distribution (around 3 km and 5.5 km) in both storm height and reflectivity distributions. The observed drier mid-troposphere, more stable layers in the lower troposphere, small TCWV, and strong downdrafts results in a higher occurrence of shallow systems during the NEM than the SWM.
- During the wet spells, the occurrence and rain fraction changes of different rain types are minimal in both seasons and seas. The prevalence of deeper systems than shallow systems is due to changes in atmospheric background conditions from dry spells to wet spells. Compared to the dry spells, the moist mid-troposphere, updrafts in the lower and mid-troposphere, the absence of lower tropospheric stable layers, and large TCWV favor the vertical growth of precipitating systems that result in more occurrences of deeper systems during the wet spells of both seasons.
- The reflectivity distributions in a given spell show the occurrence of shallow rain is larger in NEM than in SWM. The CFADs of reflectivity also show broader distributions indicating the wider distributions with large rain rates in the wet spells than dry spells during both seasons.
- The storm heights over BOB show unimodal distribution (peak at ~6 km) during the wet spells of both seasons and dry spells of SWM, while bimodal distribution (peaks at ~3 km and ~6 km) during the dry spell of NEM. Over the AS, unimodal distributions peaked at ~6 km in wet, and ~3 km in dry spells of both seasons. The storm height distributions show the occurrence of the deep systems is more in the wet spells than in the dry spells over both seas, and regardless of the spell, the occurrence of deep systems is more and shallow systems is less over BOB than over AS.
- The latent heating distributions are broader in SWM than NEM in both spells of two basins (AS and BOB). The bimodal distribution is seen in the median latent heating profile in the dry spells over AS in both SWM and NEM, and only in NEM over BOB is the resultant of higher occurrence of shallow rain in those spells.

Acknowledgements The authors would like to thank the Prof. Robert Houze and his team for providing three dimensional interpolated gridded TRMM-PR dataset (http://trmm.atmos.washington.edu/) and Copernicus Climate Change Service (C3S), for providing ERA5: Fifth generation of ECMWF atmospheric reanalysis of the global climate, dataset. (https://cds.climate.copernicus.eu/cdsapp#!/home). One of the authors Dr. K. Saikranthi would like to thank Department of Science & Technology (DST), India for providing the financial support through

the reference number DST/INSPIRE/04/2017/001185. The authors would thank the three anonymous reviewers and Editor Jianping Li for their constructive comments.

References

Ajayamohan RS, Khouider B, Majda AJ, Deng Q (2016) Role of stratiform heating on the organization of convection over the monsoon trough. Clim Dyn 47:3641–3660

Awaka J, Iguchi T, Okamoto K (2009) TRMM PR standard algorithm 2A23 and its performance on bright band detection. J Meteorol Soc Jpn 87A:31–52

Bhat GS, Kumar S (2015) Vertical structure of cumulonimbus towers and intense convective clouds over the South Asian region during the summer monsoon season. J Geophys Res Atmos 120:1710–1722

Chattopadhyay R, Goswami BN, Sahai AK, Fraedrich K (2009) Role of stratiform rainfall in modifying the northward propagation of monsoon intraseasonal oscillation. J Geophys Res Atmos 114:D19114. https://doi.org/10.1029/2009JD011869

Chen Q, Fan J, Hagos S, Gustafson WI Jr, Berg LK (2015) Roles of wind shear at different vertical levels: Cloud system organization and properties. J Geophys Res Atmos 120:6551–6574

Copernicus Climate Change Service (C3S) (2017) ERA5: Fifth generation of ECMWF atmospheric reanalyses of the global climate. Copernicus Climate Change Service Climate Data Store (CDS), date *of access*. https://cds.climate.copernicus.eu/cdsapp#!/home

Gadgil S (2003) The Indian monsoon and its variability. Annu Rev Earth Planet Sci 31:429–467. https://doi.org/10.1146/annurev.earth.31.100901.141251

Gadgil S, Joseph PV, Joshi NV (1984) Ocean atmosphere coupling over monsoonal regions. Nature 312:141–143

Goswami BN, Wu G, Yasunari T (2006) Annual cycle, intraseasonal oscillations and roadblock to seasonal predictability of the Asian summer monsoon. J Climate 19:5078–5099

Houze RA Jr, Rasmussen KL, Zuluaga MD, Brodzik SR (2015) The variable nature of convection in the tropics and subtropics: a legacy of 16 years of the Tropical Rainfall Measuring Mission (TRMM) satellite. Rev Geophys 53:994–1021. https://doi.org/10.1002/2015RG000488

Houze Jr RA, Wilton DC, Smull BF (2007) Monsoon convection in the Himalayan region as seen by the TRMM Precipitation Radar. Q J R Meteorol Soc 133:1389–1411

Karmakar N, Krishnamurti TN (2019) Characteristics of north-ward propagating intraseasonal oscillation in the Indian summer monsoon. Clim Dyn 52:1903–1916

Karmakar N, Misra V (2020) Differences in northward propagation of convection over the Arabian Sea and Bay of Bengal during boreal summer. J Geophys Res Atmos 125:e2019JD031648, https://doi.org/10.1029/2019JD031648

Karmakar N, Chakraborty A, Nanjundiah RS (2017) Space-time evolution of the low- and high-frequency intraseasonal modes of the Indian summer monsoon. Mon Weather Rev 145:413–435

Krishnamurthy V, Goswami BN (2000) Indian monsoon–ENSO relationship on interdecadal timescale. J Clim 13:579–595. https://doi.org/10.1175/1520-0442(2000)013<0579:IMEROI>2.0.CO;2

Krishnan R, Zhang C, Sugi M (2000) Dynamics of breaks in the Indian summer monsoon. J Atmos Sci 57:1354–1372

Liu C, Shige S, Takayabu YN, Zipser E (2015) Latent heating contribution from precipitation systems with different sizes, depths, and intensities in the tropics. J Clim 28:186–203

Mukhopadhyay P, Taraphdar S, Goswami BN, Krishnakumar K (2010) Indian summer monsoon precipitation climatology in a high-resolution regional climate model: Impacts of convective parameterization on systematic biases. Wea Forecasting 25:369–387. https://doi.org/10.1175/ 2009WAF2222320.1

Pathak A, Ghosh S, Kumar P, Murtugudde R (2017) Role of Oceanic and Terrestrial Atmospheric Moisture Sources in Intraseasonal Variability of Indian Summer Monsoon Rainfall. Sci Rep 7:12729

Phadtare J, Bhat GS (2019) Characteristics of deep cloud systems under weak and strong synoptic forcing during the Indian summer monsoon season. Mon Weather Rev 147:3741–3758

Radhakrishna B, Rao TN (2021) Diurnal variation of rainfall in the presence of large- and small-scale precipitating systems during different monsoon seasons over a complex terrain (Gadanki) region. J Appl Meteorol Climatol 60:857–872. https://doi.org/10.1175/JAMC-D-20-0269.1

Radhakrishna B, Rao TN, Saikranthi K (2019) Spatial coherence of water vapor and rainfall over the Indian subcontinent during different monsoon seasons. J Hydrometeorol 20:45–58. https://doi.org/10.1175/JHM-D-18-0069.1

Rajeevan M, Gadgil S, Bhate J (2010) Active and break spells of the Indian summer monsoon. J Earth Syst Sci 119:229–247

Rajeevan M, Unnikrishnan C, Bhate J, Kumar NK, Sreekala PP (2012) Northeast monsoon over India: variability and prediction. Meteorol Appl 19:226–236

Rao YP (1976) Southwest monsoon. Met Monograph, No 1. Ind Met Dept

Rao TN, Saikranthi K, Radhakrishna B, Rao SVB (2016) Differences in the climatological characteristics of precipitation between active and break spells of the Indian Summer Monsoon. J Clim 29:7797–7814

Reynolds RW, Smith TM, Liu C, Chelton DB, Casey KS, Schlax MG (2007) Daily high-resolution-blended analyses for sea surface temperature. J Clim 20:5473–5496

Romatschke U, Houze RA (2011) Characteristics of precipitating convective systems in the South Asian monsoon. J Hydrometeorol 12:3–26

Romatschke U, Medina S, Houze RA (2010) Regional, seasonal, and diurnal variations of extreme convection in the South Asian region. J Clim 23:419–439

Rowe AK, Houze RA, Brodzik S, Zuluaga MD (2019) The diurnal and microphysical characteristics of MJO rain events during DYNAMO. J Atmos Sci 76:1975–1988

Sabeerali CT, Dandi AR, Dhakate A, Salunke K, Mahapatra S, Rao SA (2013) Simulation of boreal summer intraseasonal oscillations in the latest CMIP5 coupled GCMs. J Geophys Res Atmos 118:4401–4420. doi:https://doi.org/10.1002/jgrd.50403

Saikranthi K, Rao TN, Radhakrishna B, Rao SVB (2013) Impact of misrepresentation of freezing level height by TRMM on shallow rain statistics over India and adjoining oceans. J Appl Meteorol Climatol 52:2001–2008

Saikranthi K, Rao TN, Radhakrishna B, Rao SVB (2014) Morphology of the vertical structure of precipitation over India and adjoining oceans based on long-term measurements of TRMMPR. J Geophys Res Atmos 119:8433–8449. doi:https://doi.org/10.1002/2014JD021774

Saikranthi K, Radhakrishna B, Satheesh SK, Rao TN (2018) Spatial variation of different rain systems during El Niño and La Niña periods over India and adjoining ocean. Clim Dyn 50:3671–3685

Saikranthi K, Radhakrishna B, Rao TN, Satheesh SK (2019a) Differences in the association of sea surface temperature – precipitating systems over the Bay of Bengal and the Arabian Sea during southwest monsoon season. Int J Climatol 39:4305–4312

Saikranthi K, Radhakrishna B, Rao TN, Satheesh SK (2019b) Variability in vertical structure of precipitation with sea surface temperature over the Arabian Sea and the Bay of Bengal as inferred by Tropical Rainfall Measuring Mission precipitation radar measurements. Atmos Chem Phys 19:10423–10432

Sengupta A, Nigam S (2019) The northeast winter monsoon over the Indian subcontinent and Southeast Asia: Evolution, interannual variability, and model simulations. J Clim 32:231–249

Shige S, Kummerow CD (2016) Precipitation-top heights of heavy orographic rainfall in the Asian monsoon region. J Atmos Sci 73:3009–3024

Shige S, Takayabu YN, Tao WK, Johnson DE (2004) Spectral retrieval of latent heating profiles from TRMM PR data. Part I: Development of a model-based algorithm. J Appl Meteorol 43:1095–1113

Shrestha D, Singh P, Nakamura K (2012) Spatiotemporal variation of rainfall over the central Himalayan region revealed by TRMM precipitation radar. J Geophys Res 117:D22106. doi:https://doi.org/10.1029/2012JD018140

Singh C (2013) Characteristics of monsoon breaks and intraseasonal oscillations over central India during the last half century. Atmos Res 128:120–128

Singh P, Nakamura K (2010) Diurnal variation in summer monsoon precipitation during active and break periods over central India and southern Himalayan foothills. J Geophys Res 115:D12122. doi:https://doi.org/10.1029/2009JD012794

Suhas E, Neena J, Goswami BN (2012) Interannual variability of Indian summer monsoon arising from interactions between seasonal mean and intraseasonal oscillations. J Atmos Sci 69:1761–1774

Tao W, Smith EA, Adler RF, Haddad ZS, Hou AY, Iguchi T, Kakar R, Krishnamurti TN, Kummerow CD, Lang S, Meneghini R, Nakamura K, Nakazawa T, Okamoto K, Olson WS, Satoh S, Shige S, Simpson J, Takayabu Y, Tripoli GJ, Yang S (2006) Retrieval of latent heating from TRMM measurements. Bull Am Meteorol Soc 87:1555–1572. https://doi.org/10.1175/BAMS-87-11-1555

Wallace JM, Hobbs PV (2006) Atmospheric science: An introductory survey. Second edition, Academic press, 85 pp.

Webster PJ, Magana VO, Palmer TN, Shukla J, Tomas RA, Yanai M, Yasunari T (1998) Monsoons: Processes, predictability, and the prospects for prediction. J Geophys Res Atmos 103:14451–14510. https://doi.org/10.1029/97JC02719

Zagrodnik JP, Jiang H (2014) Rainfall, convection and latent heating distributions in rapidly intensifying tropical cyclones. J Atmos Sci 71:2789–2809. https://doi.org/10.1175/JAS-D-13-0314.1